Table 3. Effect of *p*H on inhibition by pectin of heat coagulation of protein from pea stem.

*p*H	Coagulum (mg dry wt.)	
	Without pectin	With 100 μg/ml pectin
5.0	2.8	2.3
5.5	2.7	0.0
6.0	2.5	0.2
6.5	2.1	0.3
7.0	0.2	0.2

coagulation in the lower *p*H range. If the citrus pectin was boiled before it was added to the homogenate, there was no effect on protein coagulation.

From the quantitative data on ovalbumin and bovine serum albumin, whose molecular weights are known, minimal effective molar ratios were calculated for the interaction of pectin and protein. These calculations indicate that considerably less than one pectin molecule is required for interaction with one protein molecule. However, in view of the polydisperse nature of the commercial pectin employed, additional purification is required before an exact ratio can be calculated.

Although pectins are generally believed to be localized in cell walls, they may in fact also be present in the cytoplasm. If they are, the interaction of pectin and protein described here might be physiologically significant and could explain the effects of auxin on cytoplasmic viscosity and on cyclosis (*5*). It must be noted also that the fraction here designated as "cold water soluble pectin," after Albersheim and Bonner (*2*), has not been rigorously demonstrated to be polymerized methyl galacturonate, but could as well be a hemicellulose (*6*).

ARTHUR W. GALSTON
RAVINDAR KAUR
Department of Biology, Yale University, New Haven, Connecticut

References and Notes

1. A. W. Galston and R. Kaur. *Proc. Natl. Acad. Sci. U.S.* **45**, 1587 (1959); in *Plant Growth Regulation* (Iowa State Univ. Press, Ames, Iowa, 1961), p. 355.
2. P. Albersheim and J. Bonner, *J. Biol. Chem.* **234**, 3105 (1959).
3. E. A. McComb and R. M. McCready, *Anal. Chem.* **24**, 1630 (1952).
4. We thank Dr. E. F. Jansen of the Western Regional Research Laboratory of the U.S. Department of Agriculture, Albany, Calif., for a generous gift of polygalacturonase.
5. B. M. Sweeney and K. V. Thimann, *J. Gen. Physiol.* **21**, 439 (1938); ——, *ibid.* **25**, 841 (1942); H. T. Northen, *Biodynamica* **3**, 10 (1940);——, *Botan. Gaz.* **103**, 668 (1942).
6. Supported by grants from the National Science Foundation and the American Cancer Society.

10 September 1962

Embryogenesis of the Human Temporomandibular Joint

Abstract. The structures of this articulation were found to originate from two different blastemata situated at some distance from each other and operating at different rates and opposing directions. A condylar blastema evolving dorsally contributes to the formation of the condylar cartilage, the disc, the aponeurosis of the external pterygoid muscle, and the capsular elements of the lower joint level, while a temporal blastema develops the articular structures of the upper level in a forward direction. At the end of the fourth fetal month all joint elements including a glenoid fossa and articular eminence are present in their primitive form.

Recently experimental evidence has been presented to show that the condylar cartilage growth center, in contrast to epiphyseal plates of long bones, responded to induced stresses by adaptive growth movements (*1*). This unique behavior of condylar cartilage was thought to be related to its ontogenetic pattern whose details, however, are little known (*2*). In order to assess it systematically in adequate human material, the heads of 25 human fetuses of ascending stages from 15 mm CR (crown to rump) length to full term have been prepared for histologic analysis in either the coronal or sagittal plane (6 μ paraffin serial sections).

The condylar blastema appears in the form of a mesenchymal cell condensation at the dorsal end of the dentary in the 24 mm fetus. This bilateral anlage of the future mandible, the dentary, starts to ossify in the symphyseal integument at the 19 mm stage. In the 35 mm fetus it has developed dorsally and medially, in relationship to the Meckel's cartilage and the primordium of the external pterygoid muscle (Fig. 1). At the 55 mm stage, it produces an osseous head (Fig. 2) and matures at the 60 mm stage when condylar cartilage is differentiated. Simultaneously secondary cartilage also appears at the sites of the aponeuroses of the masticatory muscles. This growth spurt of the mandible coincides chronologically with that of the prechordal segment of the cranial base (*3*). While a paramedian portion of the Meckel's cartilage is incorporated into the mandibular body by a process of endochondral ossification and the secondary cartilages also disappear, the condylar cartilage starts endochondral ossification at the 85 mm stage to become henceforth the growth center of the mandible.

The evolution of the temporal blastema lags in time and space behind the condylar blastema. The first anlage is seen at the 35 mm stage in connection with the intramembranous ossification of a squamotemporal bone rod (Fig 1). At the 50 mm stage, in the region of the auditory meatus, the first temporal joint structures are differentiated in the

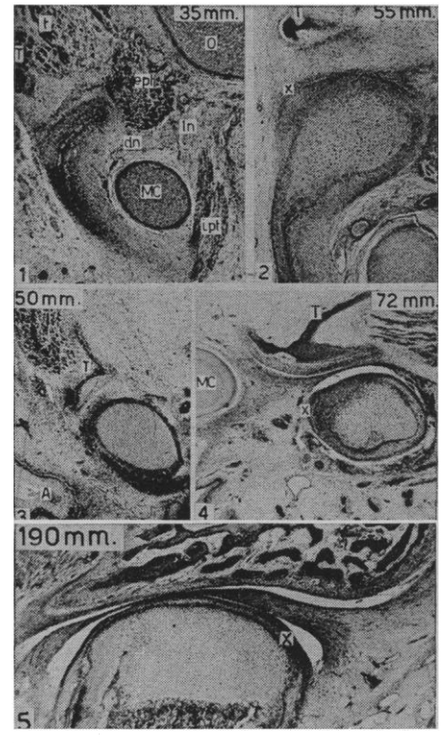

Fig. 1. Coronal section of a 35 mm CR human fetus shows condylar blastema at the level of the orbitosphenoid cartilage (*O*) and above the Meckel's cartilage (*MC*). Note beginning of intramembranous ossification of squamotemporal rod (*T*); *t*, temporal muscle; *ept*, external pterygoid muscle; *ipt*, internal pterygoid muscle; *ln*, lingual nerve; *dn*, inferior dental nerve (× 56). Fig. 2. Coronal section of a 55 mm CR human fetus shows formation of an osseous condylar head. Incipient chondrogenesis is seen at the dorsolateral aspect (*x*). Note relative aplasia of temporal blastema (*T*) at this level (× 56). Fig. 3. Coronal section of a 50 mm CR human fetus shows evolution of the temporal blastema (*T*) situated dorsally to the condylar blastema (*T*) at the level of the external auditory meatus (*A*) (× 56). Fig. 4. A sagittal section of a 72 mm human fetus shows that the temporal joint elements develop in a forward direction and the condylar elements, including the lower glenoid cavity and disc, in a backward direction as indicated by (*x*), center of most active chondrogenesis (× 36). Fig. 5. In a sagittal section of a 190 mm human fetus all articular elements are present. Condylar cartilage proliferation proceeds dorsally (*x*) while the temporal joint structures develop in a forward direction (× 36).

form of a horizontal bony plate and a thinning of the tissue below it, indicating the future upper joint cavity (Fig. 3). Further differentiation proceeds in an anterior direction to reach, at the 72 mm stage, the level of the condyle (Fig. 4). As both blastemata keep growing in opposite directions, the joint is fully formed at the 190 mm stage (Fig. 5).

Full differentiation of all articular elements by the fourth fetal month is an amazing fact which, however, is in keeping with the general embryogenetic law that at this stage all vital organs have been formed. The temporomandibular joint, according to its early histodifferentiation, would appear to be a vital organ. The condylar cartilage represents a specific growth center which develops independently from the skeletal cartilage primordium which gives rise to epiphyseal plates and basicranial synchondroses.

L. J. BAUME
Institute of Dental Medicine,
University of Geneva,
Geneva, Switzerland

References

1. L. J. Baume, *Science* **134**, 53 (1961).
2. N. B. B. Symons, *J. Anat.* **86**, 326 (1952); W. J. Hamilton, J. D. Boyd, H. V. Mossman, *Human Embryology* (Heffer, Cambridge, England, 1959).
3. E. H. R. Ford, *J. Anat.* **90**, 63 (1956).

8 August 1962

Muscle Action Potentials: A Technique for Recording in situ

Abstract. Heart tissue in situ has been immobilized with a negative pressure device, and transmembrane potentials of one cell have been observed for more than 30 minutes.

The action potential of a contractile tissue begins before the associated mechanical event. This circumstance enables an investigator to use capillary microelectrodes to record and observe a portion of the transmembrane action potential. Continuous observation is often hindered after the onset of the mechanical event when the electrode begins to slip out of the cell, loses its tip, or tears the cell membrane. The impalement procedure must then be repeated.

Better records can be obtained by inhibiting tissue motion (*1*) or by permitting the electrode to move with the cell (*2*). A local area of the surface of cardiac muscle has been immobilized

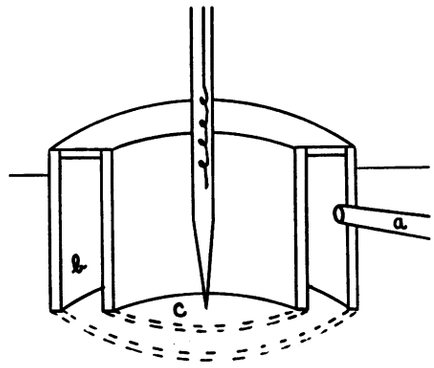

Fig. 1. Negative pressure holding device.

by a negative air pressure device, which restrains the tissue so that a standard microelectrode can then be maintained within a cell for more than 30 minutes. In the ring-shaped device, shown in Fig. 1, the central area *c* is open for penetration of a microelectrode from above. The holding ability varies directly with the total grasping area and with the degree of negative pressure introduced into the volume (*b*). The glass tube (*a*) is both the mechanical support and the negative pressure line. The diameter of the central area should be kept as small as possible. For the frog heart, a central diameter of less than 2 mm and a negative pressure of less than 10 cm of water was used.

A laboratory vacuum line was the source of negative pressure. A large capacity bleeder valve determined the degree of negative pressure developed at the tissue holder. The line between the bleeder valve and the holder was monitored by a water manometer. After preliminary adjustment of the pressure, the exhaust line was temporarily clamped shut while the device was brought firmly into contact with the heart, at which moment the line was opened. Intermittent grasping was reflected by movements of the water level of the manometer during the cardiac contraction cycle. The glass microelectrode was held in a Pfeiffer manipulator.

Figure 2 (*a* and *b*) shows the intracellular potentials recorded in situ from a ventricle of *Rana pipiens*. The reference electrode, a chlorided silver wire, was placed in the lower abdominal cavity. The dip in the base line between action potentials, usually present during recordings in situ, represents the effect of volume conductor currents on the reference electrode (*2*). At the end of 45 minutes, the action potential amplitude and duration have decreased, and the heart rate has become slower.

The negative pressure technique was used for transmembrane recordings from the heart of *Limulus polyphemus*, in situ. The upper trace of Fig. 2*c* is the microelectrode recording. The lower trace represents the motion of an adjoining area of heart. The motion transducer was a piezoelectric device loaded by the 1000 megohm input of a preamplifier (Bioelectronics). The time constant was greater than 5 seconds. Transient electrical activity began before muscle movement. The fast rising small waves are not motion artifact. Surface recordings made with a string galvanometer and liquid electrodes exhibit similar contours and the expected reverse polarity (*3*). Garrey has presented reasons for considering the small potentials to be biogenic and McCann agrees that these are bioelectric potentials (*4*).

The immobilizing devices were made of plastic tubing. For best results, the tissue holder dimensions should be appropriate for the particular type of

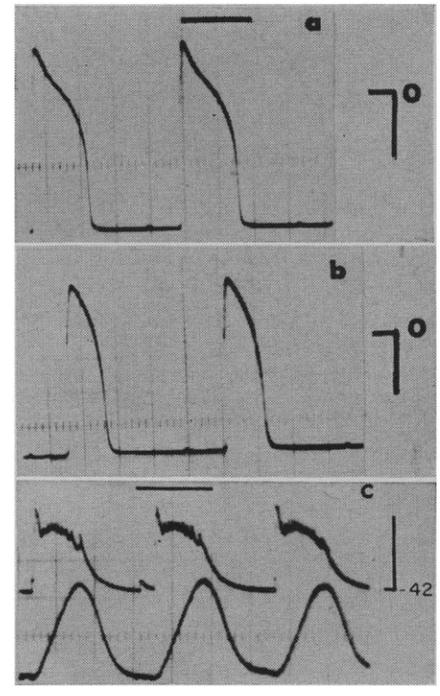

Fig. 2. In situ recordings: *a*, potentials from frog ventricle 5 minutes after impalement; *b*, 45 minutes after impalement; *c*, upper trace, transmembrane potentials from the heart of *Limulus polyphemus*; *c*, lower trace, motion of the cardiac surface. Calibration: *a* and *b*: vertical, 40 mv, horizontal, 1 sec; *c*: vertical, 20 mv, horizontal, 1 sec.